SUMMARY OF AEROTHERMAL TEST RESULTS FROM THE FIRST FLIGHT OF THE PEGASUS AIR-LAUNCHED SPACE BOOSTER

Gregory K. Noffz*
Robert E. Curry**

NASA Dryden Flight Research Facility
Edwards, California

ABSTRACT

Temperature measurements were obtained on the Pegasus® booster from launch through Mach 8.0. The majority of sensors were thin foil temperature gages installed near the surface within the vehicle's ablating thermal protection system. These gages were distributed on the wing surfaces and on the wing-body fairing or fillet. Temperature time histories from these installations are presented. In addition, thermocouples were installed on the surface of nonablating plugs located on the fairing. These sensors were more responsive to changes in flight conditions than the foil gages and allowed a derivation of convective heat flux. A heating rate magnification of 2 was found in the vicinity of the wing shock interaction.

NOMENCLATURE

c	local wing chord, in.
c_p	specific heat, Btu lb_m^{-1} °F^{-1}
FS	fuselage station, in.
$Heat_{abl}$	heat of ablation, Btu lb_m^{-1}
HRSI	high-temperature reusable surface insulation
h	pressure altitude, ft
k	thermal conductivity, Btu ft^{-1} hr^{-1} °F^{-1}
LTA	Lockheed Thermal Analyzer
M_∞	free-stream Mach number
NASA	National Aeronautics and Space Administration
q	heat flux, Btu ft^{-2} sec^{-1}
$\bar{q}$	free-stream dynamic pressure, lb ft^{-2}
q_{cond}	conductive heat flux into wall from surface, Btu ft^{-2} sec^{-1}
q_{conv}	convective heat flux to the surface, Btu ft^{-2} sec^{-1}
q_{rad}	radiative heat flux, Btu ft^{-2} sec^{-1}
q_{ref}	reference surface convective heat flux, Btu ft^{-2} sec^{-1}
T	temperature, °F
T_{abl}	ablation temperature, °F
T_{act}	activation temperature, °F
T_s	surface temperature, °R
TC	thermocouple
TPS	thermal protection system
t	time from launch, sec
x	local longitudinal coordinate, measured aft from leading edge, in.
y	lateral coordinate, measured to the right from vehicle centerline, in.
z	vertical coordinate, measured up from vehicle thrust line, in.

Greek symbols

α	angle of attack, deg
β	angle of sideslip, deg
Δ_q	incremental difference in convective heat flux, Btu ft^{-2} sec^{-1}
ε	emissivity
ρ	density, lb_m in^{-3}
σ	Stefan-Boltzmann constant, 3.3063×10^{-15} Btu in^{-2} sec^{-1} °R^{-4}

*Aerospace Engineer.
**Aerospace Engineer. Member AIAA.

® Pegasus is a registered trademark of Orbital Sciences Corp., Fairfax, Virginia.

INTRODUCTION

The Pegasus® vehicle is an air-launched, three-stage solid rocket booster that uses a wing and conventional control surfaces at speeds up to Mach 8.0 and offers the potential for performing add-on experiments. These add-on experiments are based on the concept of small research packages that can be incorporated into a Pegasus vehicle with minimal impact to its primary orbital insertion mission. The Pegasus booster offers the advantages of being a large-scale vehicle with a large amount of internal volume in the first stage. In addition, approximately every 16 lb added to the first stage reduces the orbital payload capability by only 1 lb. Some of the disadvantages of the Pegasus add-on concept are that the vehicle is nonrecoverable, has ablating surfaces, and flies a fixed trajectory. A series of add-on experiments has been proposed. On the early flights, the complexity has been limited to meet flight schedules. On later flights, more sophisticated experiments are planned to study phenomena such as crossflow-induced boundary-layer transition. The overall goal of these add-on experiments is to perform appropriate hypersonic research, given the limitations of the Pegasus vehicle.

The specific research objectives of instrumenting flights no. 1 and 2 are: (1) to develop measurement techniques on an ablating vehicle, (2) use some of these techniques to obtain in-flight temperature measurements that can be used for evaluation of analytic design tools, and (3) to obtain empirical information related to specific hypersonic flow features of the configuration.

The first objective deals with obtaining useful aerothermal measurements on an ablating vehicle, such as the Pegasus booster, which has a thermal protection system (TPS) consisting of thin layers of ablative and insulative materials. Two types of temperature sensors were installed and tested. Foil temperature gages offered the possibility of measuring temperatures between the thin layers of thermal protection with minimal perturbation. Nonablating plugs with thermocouples (TCs) at the surface were installed in the wing-body fillet region. The plugs were fabricated from high temperature reusable surface insulation (HRSI). The HRSI material, originally developed for the space shuttle, offered a well-defined insulation in terms of material properties and characteristics.

The second objective was to obtain flight data that can be used for the evaluation of analytical design tools. During the development phase, the Pegasus configuration was never tested in a wind tunnel, resulting in substantial savings in time and cost.[1] Such an approach, however, required heavy reliance upon analytic tools used in the aerodynamic and thermal protection design process. The flight no. 1 research system included temperature sensors distributed on the wing surfaces, leading edge, and the wing-body fairing (or fillet). These sensors were intended to provide direct measurements for comparison with analytic predictions.

The third objective was to obtain empirical information about certain aerothermal features of the configuration, particularly additional heating caused by wing shock in the vicinity of the fillet. Because of the variation of Mach number and angle of attack during the flight, a wide range of wing-body flow conditions were present. The distribution of the plug-mounted sensors was selected to identify the effects of the shock wave and compression field generated by the wing. The surface temperatures on the plugs were expected to respond rapidly to these local aerothermal conditions and were used to derive estimates of convective heat flux.

This paper presents the results of the flight no. 1 instrumentation effort. Presented in the results section are typical temperature time histories measured within the TPS and also chordwise temperature distributions for some of the wing installations. The usefulness of the foil gages and HRSI plugs for temperature measurement, as well as the derivation of heat flux, will be discussed.

The authors would like to acknowledge the financial support of the Defense Advanced Research Projects Agency (DARPA).

TEST APPARATUS

Vehicle Description

The Pegasus vehicle is an air-launched, winged, three-stage expendable solid rocket booster system intended to deliver payloads of up to 900 lb into low Earth orbit. The launch configuration is shown in Fig. 1, along with a photograph of the booster mated to the B-52 carrier aircraft. The wing, tail surfaces, and wing-body fillet are all located on the first stage. Research instrumentation components described in this report were installed on the first stage of the flight no. 1 vehicle. The vehicle was approximately 49.5 ft long with a wing span of 22 ft. Total weight at launch for the flight no. 1 vehicle was 41,765 lb.

The Pegasus wing is nearly triangular in planform with zero dihedral and 45° leading-edge sweep. The airfoil sections at lateral coordinate (y) = 65 in. and y = 32 in. are shown in Figs. 2(a) and (b), respectively. The airfoil is a truncated diamond type with a nominal 1-in.-radius leading edge. The wing skin structure is constructed of foam sandwiched between two 0.040-in.-thick layers of graphite-epoxy. The wing leading edge is constructed of solid graphite-epoxy and has a nominal thickness of 0.125 in.

The wing-body fillet provides an aerodynamic fairing between the wing and the cylindrical rocket motor casing that forms the fuselage. The fillet construction is similar to that of the wing.

The Pegasus TPS consists of ablative and insulative materials in various combinations applied to the external

® Pegasus is a registered trademark of Orbital Sciences Corp., Fairfax, Virginia.

surface of the graphite-epoxy substructure. Four materials were used: Firex RX-2376A (Pfizer Minerals, Pigments and Metals Division, New York, New York), Thermolag T-230 (Thermal Science, Inc., St. Louis, Missouri), cork phenolic, and an Acurex-developed spray-on insulator (Acurex Corp., Huntsville, Alabama). Thermal properties of these materials are given in Table 1. Firex is a polymer ablator that begins to melt and flow at approximately 250 °F. Thermolag is an ablator that sublimes at a temperature of approximately 230 °F. Both ablative materials are sprayed on. Cork was obtained in 0.04-in.-thick pressed sheets and glued in place. The Acurex insulator consisted of glass microballoons suspended in an epoxy resin. Once sprayed, the insulator begins to set, and eventually hardens to a brittle foam. On the wing, Firex ablator was sprayed over the Acurex insulator; on the fillet, Thermolag ablator was applied over cork. Specific details of the TPS as applied at the various sensor installations are described in the next section.

Instrumentation

The flight no. 1 instrumentation system consisted of 86 chromel-alumel (type K) TCs and related signal conditioning hardware. On the right wing, TPS-embedded "foil" TCs were located along the leading edge, in two chordwise rows on the lower surface, and at various points on the upper surface. On the right side of the wing-body fillet, TPS-embedded foil TCs were located in a grid-like pattern as were the plug-mounted TCs. This paper will show results from the two chordwise, lower surface rows and the fillet instrumentation. A summary of sensor distribution is given in Table 2. Figures 4 and 5 contain precise sensor locations and will be discussed in this section.

The majority of TCs (61) were foil types approximately 0.006 in. thick and encased in a polyimide laminate, see Fig. 3(a). These sensors provided temperature time histories between the various layers of thermal protection with a minimum amount of disturbance to the TPS. The only modification required to the structure is a 0.187-in. hole at each location for the TC leads to be routed through.

Ten type-K TCs were fabricated from small-diameter (0.005-in.) wires which were mounted on the surface of 1-in.-diameter, 0.4-in.-thick plugs, see Fig. 3(b). The plugs were solid pieces of shuttle tile material, LI2200 (also known as HRSI). Details of the material properties are given in Table 3. A high-temperature, high-emissivity coating was applied over the plugs including the TCs. The emissivity of the coating was measured using a spectrophotometer and was determined to be 0.85. Samples of the coating were heated in ground facilities to temperatures of 600 °F and no degradation in emissivity was observed. Indentations had to be provided in the structure to allow flush-mounting of the plugs. Consequently, the structure is perturbed far more than in the case of the foil gages, but the HRSI plugs provide a reliable way to estimate heat flux at the surface as will be seen in a later section.

Wing Foil Thermocouple Installations

Twenty-six TCs (24 thin foil TCs and 2 standard bulb types) were installed in the wing lower surface TPS. The TPS design for the wing surfaces consisted of a 0.040-in. layer of Acurex insulator and an external layer of 0.015-in. Firex ablator. See Fig. 4 for wing sensor locations and local TPS configuration.

Fillet Installations

All fillet instrumentation locations are diagramed in Fig. 5 and include foil gages installed within the TPS and HRSI plug installations. On the fillet, the TPS consisted of Thermolag ablator 0.015 in. thick sprayed over a 0.040-in. layer of cork insulator. The fillet TCs are installed in much the same way as those on the wing.

FLIGHT CONDITIONS AND TRAJECTORY

No onboard airdata measurements were taken on the Pegasus vehicle. Therefore, free-stream airdata quantities were estimated postflight by a combination of inertial data from an onboard inertial navigation system (INS), atmospheric data from balloons, stratospheric charts, climatological information, and seven ground-based radar tracking sites.[2]

Flight condition parameters from release to first-stage separation are shown in Figs. 6(a) and (b). The Pegasus vehicle began its path to orbit under the right wing of the NASA B-52 aircraft. Launched from 40,000 ft, the Pegasus booster drops away from the bomber for approximately 5 sec before the first stage ignites, Fig. 6(a). A 2-g pullup is then executed, during which the vehicle reaches a maximum angle of attack of approximately 20°, Fig. 6(b). Angle of attack is reduced to approximately 8° from approximately Mach 2.0 to Mach 3.5. Angle of attack is near 0° for the remainder of first-stage flight. Maximum dynamic pressure is approximately 850 lb ft^{-2} and occurs 30 sec after launch, Fig. 6(a). At that time, altitude is just under 60,000 ft and Mach number is approximately 2.5. Angle of sideslip is given in Fig. 6(b).

HEAT FLUX DERIVATION FROM NONABLATING PLUGS

The HRSI plugs were modeled analytically using the Lockheed Thermal Analyzer (LTA) program, a finite difference code that solves transient thermal problems in up to three dimensions (Lockheed Report 18902, *Thermal Analyzer Computer Program for the Solution of General Heat Transfer Problems*). The LTA program was used to determine the conduction and radiation components from the temperature time histories measured at the plug surfaces.

Because of a plug's large width, temperature measured at the center of the surface is considered unaffected by edge

conditions and a one-dimensional, finite difference thermal model sufficed. Thinner elements were used near the surface that experienced higher temperature gradients. The HRSI plugs were coated with a thin layer of black paint. The paint's conductivity was not modeled; however, its surface emissivity was taken into account. The HRSI thermal conductivity was input as a function of temperature and static pressure (Table 3). Specific heat of HRSI varied with temperature alone.

The nonablating HRSI surface experiences all three modes of heat transfer at the surface: convection, conduction, and radiation, but no energy leaves the surface in the form of ablation products. Given the surface temperature and assuming a view factor of 1.0 and a 0.0 °R reservior, radiation heat transfer was determined from the Stefan-Boltzmann equation:

$$q_{rad} = \varepsilon \sigma T_s^4$$

Using the surface temperature time history, the heat conduction into the wall can be determined from a one-dimensional finite difference model such as the one used in the LTA program, and is based on

$$q_{cond} = -k \left(\frac{dT}{dx} \right) x = 0$$

The convective heat flux at the surface is then the sum of the radiative and conductive heat fluxes,

$$q_{conv} = q_{cond} + q_{rad}$$

provided the conduction component is defined as positive when heat is flowing into the material and the radiation component is defined as positive when energy is leaving the surface. A similiar procedure was used in the analysis of space shuttle thermal data.[3]

DISCUSSION OF RESULTS

Wing Thermal Protection System

Figure 7 shows an example of temperatures measured at the same wing location but between the different layers of thermal protection. Prior to launch, all temperatures were at steady values between approximately −5 to −35 °F. At locations where multiple TCs were installed, no large temperature gradients were present across the layers of the TPS. This indicated that the TPS was cold-soaked to near atmospheric conditions and that there were no large instrumentation biases in the system. Prior to launch the graphite-epoxy inner wall is slightly warmer than the outer layers in most cases. As the flight progressed, measurable temperature differences developed between the thin thermal protection layers. As expected, the temperature rise of the lower sensors lags that of the sensor located nearest to the surface. These measurable temperature differences across the layers may allow an estimation of surface heat flux prior to the onset of ablation. This issue will be discussed later. The maximum temperature measured on the graphite-epoxy substructure never exceeded 230 °F.

Examples of the lower surface wing temperature time histories measured at the Firex–insulator interface are shown in Figs. 8(a) through (d). On the inboard row (Figs. 8(a) and (b)), all the aft locations as well as the station nearest the leading edge (fuselage station (FS) = 293 in.) level off at approximately 250 °F, the ablation temperature of Firex. The second and third stations (FS = 283 in., FS = 273 in.) exceed the data range limit of 320 °F indicating the ablative material is depleted in this area. This pattern is repeated on the outboard row (Figs. 8(c) and (d)) with the second and third stations (FS = 253 in., FS = 245 in.) exceeding the ablation temperature. The third station (FS = 245 in.) exceeds the data range limit by $t = 45$ sec.

To better visualize the phenomena seen in Fig. 8, Firex–insulator interface temperatures are plotted as a function of chord for different times in Fig. 9. As seen at the inboard (Fig. 9(a)) and outboard (Fig. 9(b)) locations, by 50 sec after launch the majority of temperatures are approaching the ablation temperature of Firex (250 °F), while temperatures between chord location $(x/c) = 0.1°$ and 0.3° continued to increase above the 250 °F level indicating that the ablative layer was depleted in this region.

Since data from the embedded TCs are expected to be sensitive to details of the sensor installation and TPS installation processes, the consistency of the trends from the two chordwise distributions is considered good. The higher temperatures observed on the outboard row at $x/c = 0.62$ may be a result of variation in thickness of the TPS layers or possibly an incomplete bond between the TC and the TPS layers.

Fillet Thermal Protection System

Figures 10(a) and (b) show examples of temperature time histories for the foil gages embedded in the fillet TPS. Initial temperatures for these sensors were similar to the wing sensors. Most of the sensors reached the ablation temperature of the Thermolag (230 °F) which is slightly lower than the wing ablative material. Although some sensors exceeded the ablation temperature, all temperatures leveled out at no more than 270 °F.

Fillet High-Temperature Reusable Surface Insulation Plugs

Examples of surface temperature and derived convective heat flux for selected HRSI plugs are shown Fig. 11. Initial temperatures of the plugs were slightly higher than the TPS values and the plug data show more fluctuations during the flight and much higher maximum temperatures. Rapid surface response to external heating variations is expected since the HRSI plugs are not covered with ablative material and have highly insulative properties. Subtle variations in the temperature time histories correspond to substantial heat flux variations. As with the foil TCs, the plugs begin to heat

up at approximately 10 sec. Temperature steadily increases for all of the plugs until approximately 45 sec as shown in Fig. 11. A large heat flux pulse is shown by all the HRSI plug data at t = 76 sec, (Fig. 11). The time and magnitude of this event is essentially the same for all plugs. This event coincides with the final seconds of first-stage motor operation when the exhaust plume expands, possibly resulting in radiative heating of the fillet.

As the Pegasus vehicle begins to experience aerodynamic heating, the surface temperatures of the plugs and of the surrounding TPS begin to rise. For the temperatures of interest (< 230 °F), the conductivity of Thermolag and HRSI are of the same order of magnitude (approximately 0.08 and 0.05 Btu ft^{-1} hr^{-1} $°F^{-1}$, see Tables 1 and 3). Thus, the surface temperatures should rise at approximately the same rate, at least until the ablation rate from the TPS becomes significant. At that point, the TPS surface temperatures level off at no more than 270 °F while the plug surface temperatures continue to rise. Until ablation starts, a rough estimate of temperatures within the TPS can be made from applying the plug-derived heat flux to an LTA model of the TPS. Figure 12 shows the TPS temperature profiles calculated by the LTA model using the derived heat flux from an HRSI plug (FS = 280.6 in., vertical coordinate (z) = 18 in.). Plotted on the same figure are the interface profiles from the foil installation just below the plug (FS = 280.6 in., z = 15.5 in.). Measured and modeled interface temperatures show good agreement considering the differences in the thermal properties between the HRSI plugs and the TPS. The calculated and measured Thermolag–cork interface temperature traces contain a slight change in slope between 25 and 32 sec. This is an indication that the foil gages are responding to the same heat flux variations as the plugs.

The derived heat flux data must be interpreted with respect to the trajectory and sensor location. By using supersonic wedge tables[4] for several trajectory flight conditions, an estimate of the wing leading-edge shock-wave position, superimposed on the sidewall of the fillet, is shown in Fig. 13(a). This estimate does not account for offsets caused by the 1-in. wing leading-edge radius or fuselage bow shock effects. Based on this estimate, however, the three sensors at the forward corner of the fillet, farthest from the wing, are expected to be upstream of the wing shock at flight conditions where aerodynamic heating is significant. When compared, heat flux data for these sensors agree favorably throughout the flight profile, see Fig. 13(b). Therefore, data from these sensors will be referred to as the reference heating, q_{ref}, and used to normalize data from other fillet sensors.

Figure 14 shows the additional heating, which is defined as:

$$\Delta_q = q_{conv} - q_{ref}$$

for two fillet sensors. These sensors are located aft and close to the lower surface of the wing, and are therefore downstream of the estimated shock position at all flight conditions. Substantial additional heating is present for these sensors during the first half of the flight. The additional heating builds to a maximum at $t \approx 46$ sec, when the angle-of-attack pitch-down maneuver begins (see Fig. 6). At $t \approx 55$ sec, this maneuver is complete, and angle of attack is approximately 0° for the remainder of the flight. Additional heating after t = 55 sec also is approximately zero.

Figure 15 shows the additional heating for the sensors located in the wing shock region. For most of these sensors, some additional heating is present during the portion of the flight with angle of attack (t < 55 sec). After t = 55 sec, when angle of attack is 0°, these sensors indicated additional heating up to approximately 0.47 Btu ft^{-2} sec^{-1}. It is hypothesized that this additional heating is caused by the proximity of the wing leading-edge shock. Other factors to be considered are the vehicle angle of sideslip and Mach number. Angle of sideslip (β) is below or near 0° during most of the high Mach number portion of the flight. During the period of peak additional heating caused by the shock, 60 < t < 70 sec, angle of sideslip approaches a value of $\beta \approx 1°$ at $t \approx 65$ sec (resulting in the right-hand side of the fillet being more windward).

Reference heating at t = 62 sec is approximately 0.5 Btu ft^{-2} sec^{-1}. The peak additional heating observed in this experiment of 0.47 Btu ft^{-2} sec^{-1} corresponds to an additional heating factor of approximately 2 ($q_{conv}/q_{ref} \approx 2$). Perhaps follow-on Pegasus experiments will better define the significance of angle-of-sideslip effects, the local pressure field, and boundary-layer characteristics in this vicinity to provide better interpretation.

CONCLUDING REMARKS

Temperature measurements within the thermal protection system (TPS) of the first Pegasus® air-launched space booster are presented. The TPS temperature measurements were obtained on the wing lower and upper surfaces and wing-body fillet. In addition, surface heat flux is calculated for the high-temperature reusable surface insulation (HRSI) plugs installed on the wing-body fillet. The data presented in this report can be used to evaluate the effectiveness of the aerothermal design tools used in the development of the Pegasus vehicle, help evaluate sensor installation concepts, and provide empirical information related to specific hypersonic flow features of the configuration.

Thin foil thermocouples installed within the thermal protection system have provided a way of obtaining temperature measurements within the thin layers of the Pegasus TPS. The nonablating HRSI plugs proved responsive to small variations in vehicle flight conditions and provided a means of deriving heat flux estimates.

® Pegasus is a registered trademark of Orbital Sciences Corp., Fairfax, Virginia.

The thin foil gage data from the wing indicated consistent trends in the inboard and outboard measurement rows. Most wing temperature time histories stabilized near the ablation temperatures, with the exception of sensors between 10 and 30 percent of the wing chord where the ablative material appears to have been depleted. The data from foil gages at lower depths in the TPS showed consistent lags because of the thermal capacitance and thermal resistance of the TPS.

Temperatures measured within the fillet TPS were generally similar to the wing data; however, no sensors significantly exceeded the ablation temperature. As expected the nonablating, highly insulative plugs experienced higher surface temperatures and showed more responsiveness to changes in flight conditions.

Derivations of convective heat flux from the HRSI plugs resulted in consistent trends for all sensors forward of the expected wing leading-edge shock position. Data obtained from sensors aft of the shock had additional heating characteristics that could be directly related to vehicle Mach number, angle of attack, and angle of sideslip. The maximum value of heating rate measured in the vicinity of the shock was approximately twice the value ahead of the shock. This additional peak heating appears to be sensitive to small variations in angle of sideslip.

REFERENCES

[1] Mendenhall, Michael R., Lesieutre, Daniel J., Caruso, Steven C., Dillenius, Marnix F.E., and Kuhn, Gary D., "Aerodynamic Design of Pegasus™: Concept to Flight with CFD," *Missile Aerodynamics* AGARD-CP-493, 1990.

[2] Noffz, Gregory K., Curry, Robert E., Haering, Edward A., Jr., and Kolodziej, Paul, *Aerothermal Test Results from the First Flight of the Pegasus Air-Launched Space Booster*, NASA TM-4330, 1991.

[3] Hartung, Lin C., and Throckmorton, David A., *Space Shuttle Entry Heating Data Book, Volume 1–STS-2*, NASA RP-1191, pt. 1, 1988.

[4] Ames Research Staff, "Equations, Tables and Charts for Compressible Flow," *Thirty-Ninth Annual Report of the National Advisory Committee for Aeronautics*, NACA Report 1135, 1953, pp. 613–681.

Table 1. Properties of TPS materials.

Material	ρ, $lb_m\ in^{-3}$	k, Btu $ft^{-1}\ hr^{-1}\ °F^{-1}$	c_p, Btu $lb_m^{-1}\ °F^{-1}$	$Heat_{abl}$, Btu lb_m^{-1}	T_{act}, °F	T_{abl}, °F	Description
Acurex insulator	0.00613	0.0258	0.262	n/a	n/a	n/a	Patterned after insulator on shuttle main tank. Microballoons in epoxy. Spray-on application.
Cork phenolic	0.0177	0.04	0.47	n/a	n/a	n/a	Multipurpose insulator. Organic fiber. Bonded in place.
Firex RX-2376A	0.04	0.14	0.4	1800	280	250	Low-temperature ablative material. Polymer. Spray-on application.
Thermolag T-230	0.0521	0.08	0.3	750	n/a	230	Low-temperature ablative material. Polymer. Spray-on application.

Table 2. Temperature sensor distribution.

	Foil gages	Bulb gages	HRSI plugs
Wing upper surface	3	2	0
Wing lower surface	25	6	0
Leading edge	15	0	0
Fillet	18	2	10
Signal conditioning equipment	0	5	0
Total	61	15	10

Table 3. HRSI material properties; HRSI density (LI-2200) = 22 lb_m in^{-3}.

(a) Transverse thermal conductivity.

	Pressure, atmosphere					
Temperature, °F	10^{-5}	10^{-4}	10^{-3}	10^{-2}	10^{-1}	1
−250	0.0133	0.0133	0.0167	0.0267	0.0300	0.0333
−150	0.0150	0.0150	0.0183	0.0283	0.0333	0.0367
75	0.0183	0.0183	0.0233	0.0333	0.0408	0.0467
500	0.0250	0.0250	0.0317	0.0408	0.0558	0.0650
1000	0.0358	0.0358	0.0442	0.0533	0.0783	0.0900

(b) Specific heat.

Temperature, °F	c_p, Btu lb_m^{-1} $°F^{-1}$
−250	0.070
−150	0.105
0	0.150
250	0.210
500	0.252
750	0.275
1000	0.288

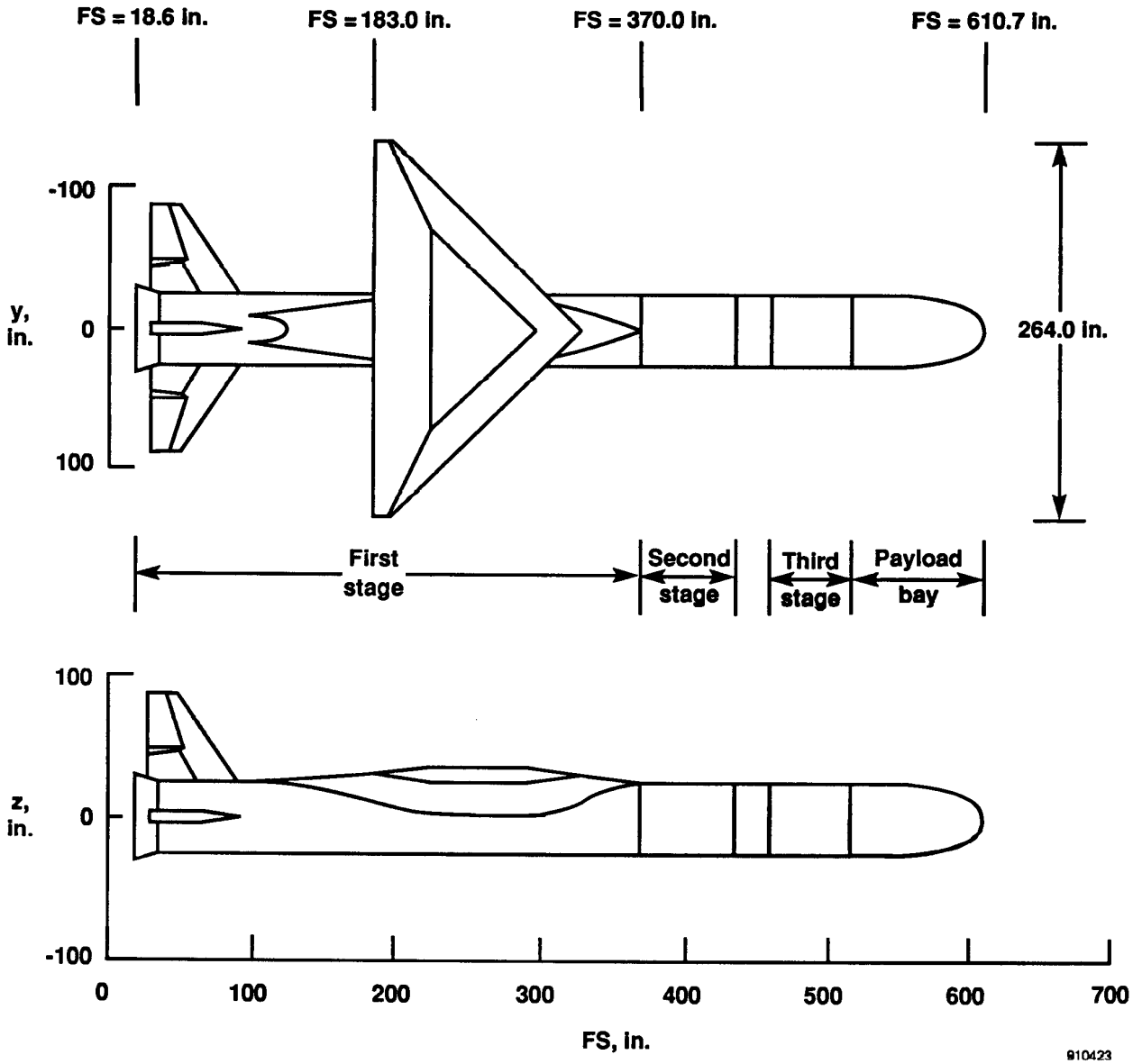

(a) Pegasus two-view.

Fig. 1 Pegasus launch configuration.

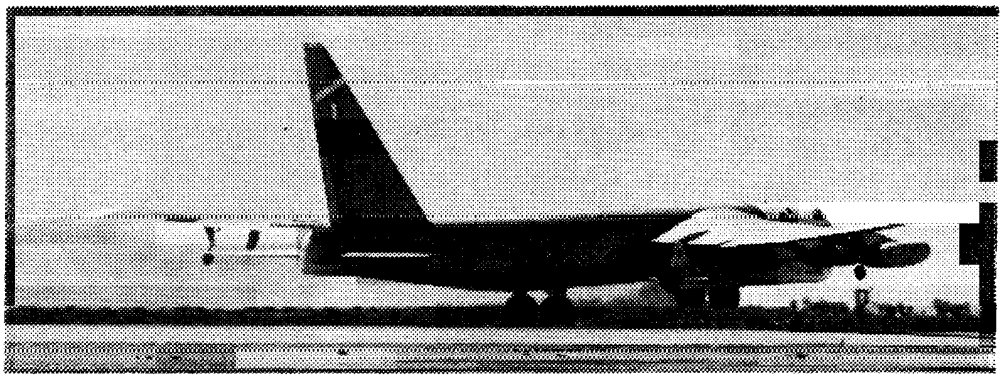

EC90 111-1

(b) B-52 carrier and Pegasus vehicle at takeoff.

Fig. 1 Concluded.

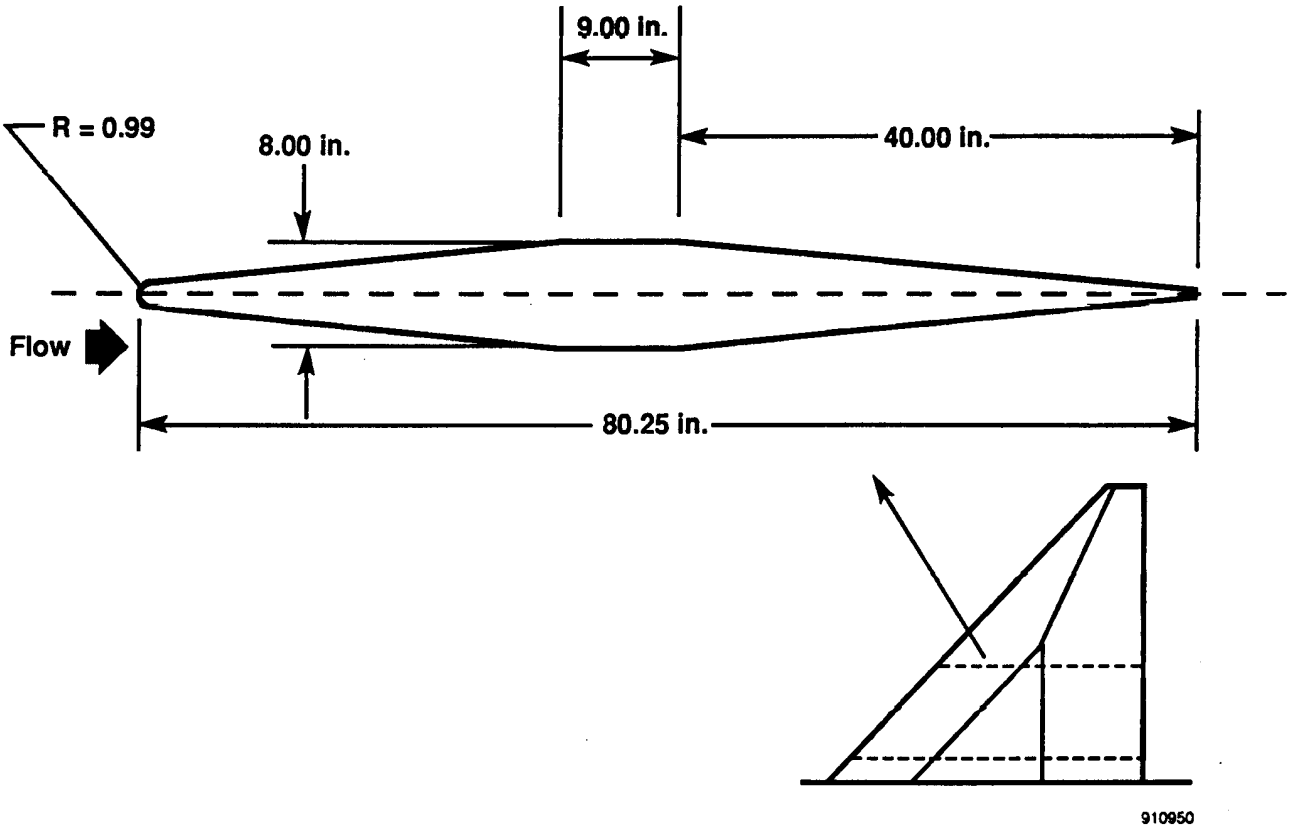

(a) Airfoil section at $y = 65$ in.

Fig. 2 Airfoil sections where temperature sensors were located.

EC90 111-1

(b) B-52 carrier and Pegasus vehicle at takeoff.

Fig. 1 Concluded.

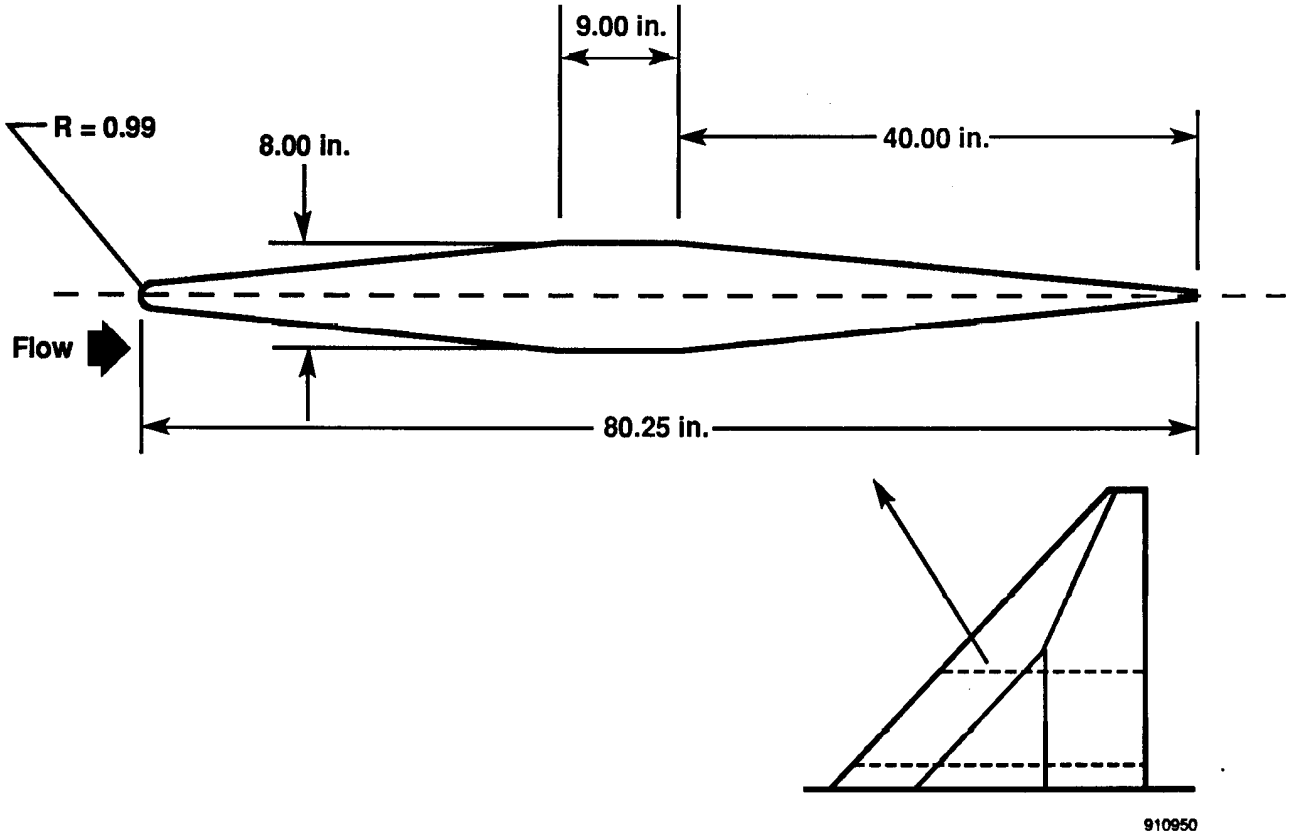

(a) Airfoil section at $y = 65$ in.

Fig. 2 Airfoil sections where temperature sensors were located.

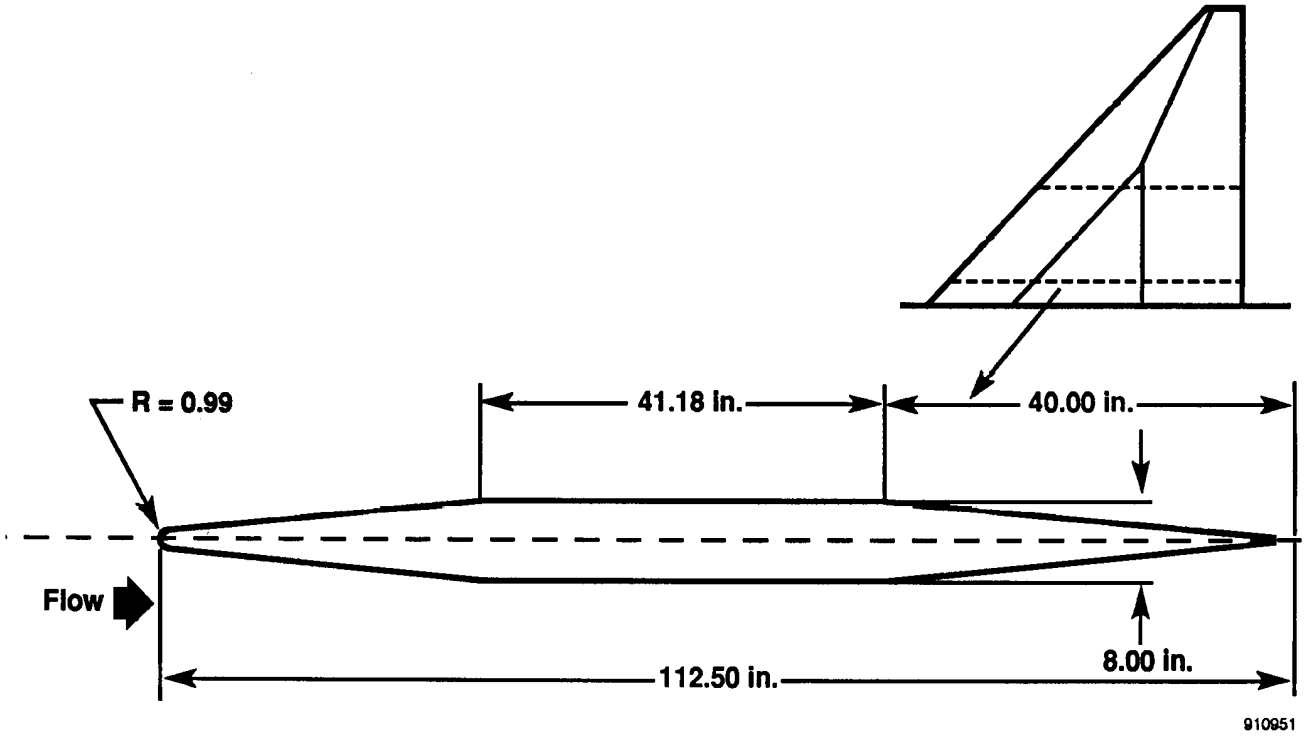

(b) Airfoil section at $y = 32$ in.

Fig. 2 Concluded.

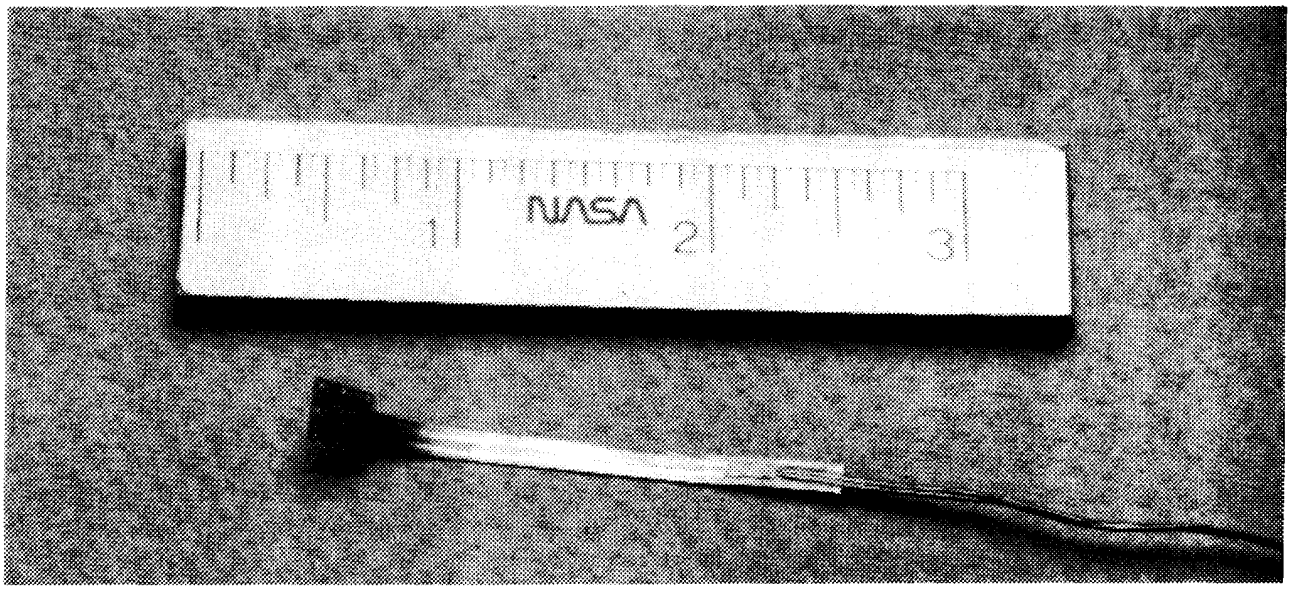

EC89 317-5

(a) Foil gage TC sensor and leads.

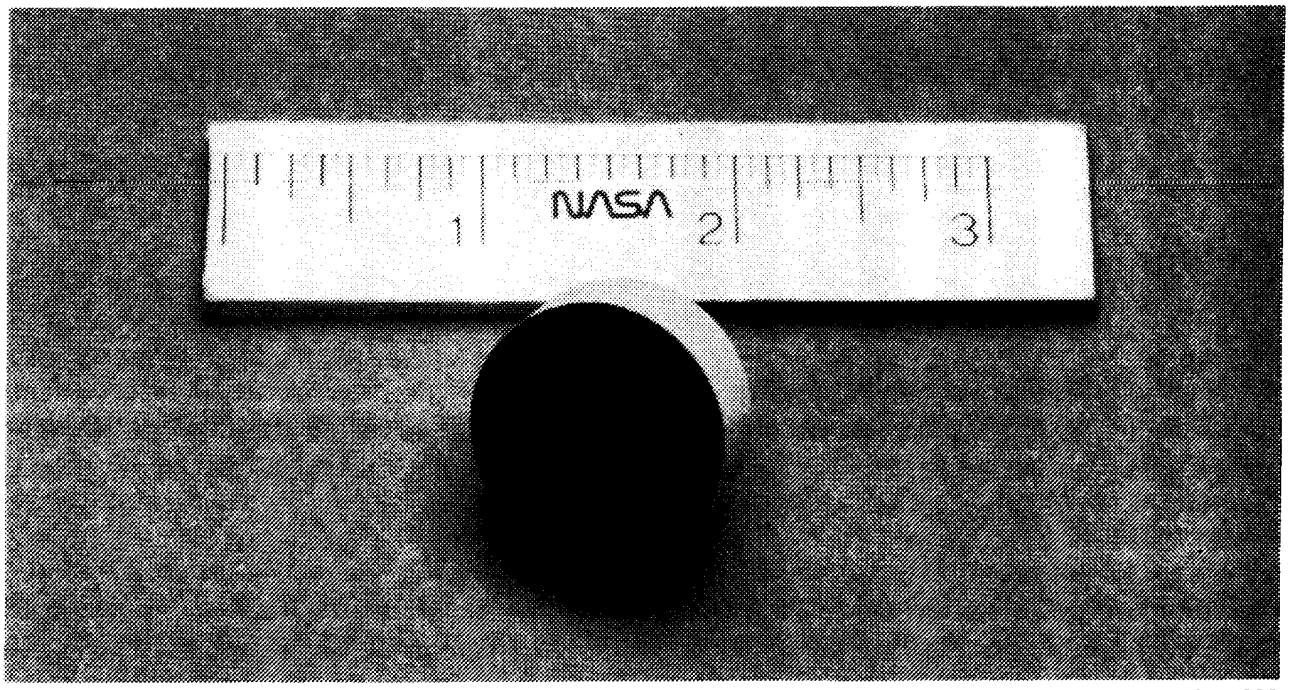

EC89 0317-003

(b) HRSI plug.

Fig. 3 Flight no. 1 instrumentation.

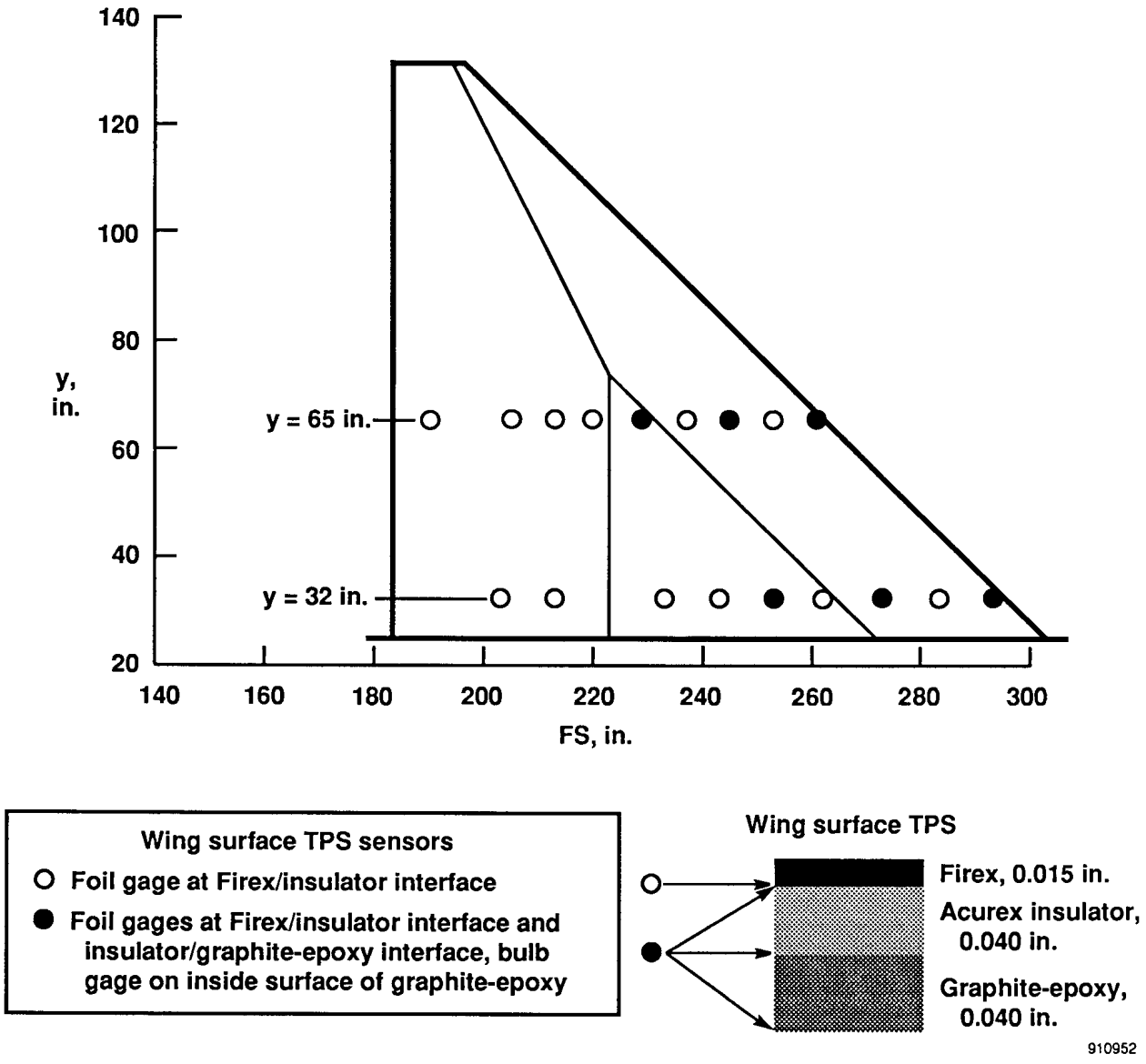

Fig. 4 Plan view of right wing lower surface, showing temperature sensor locations.

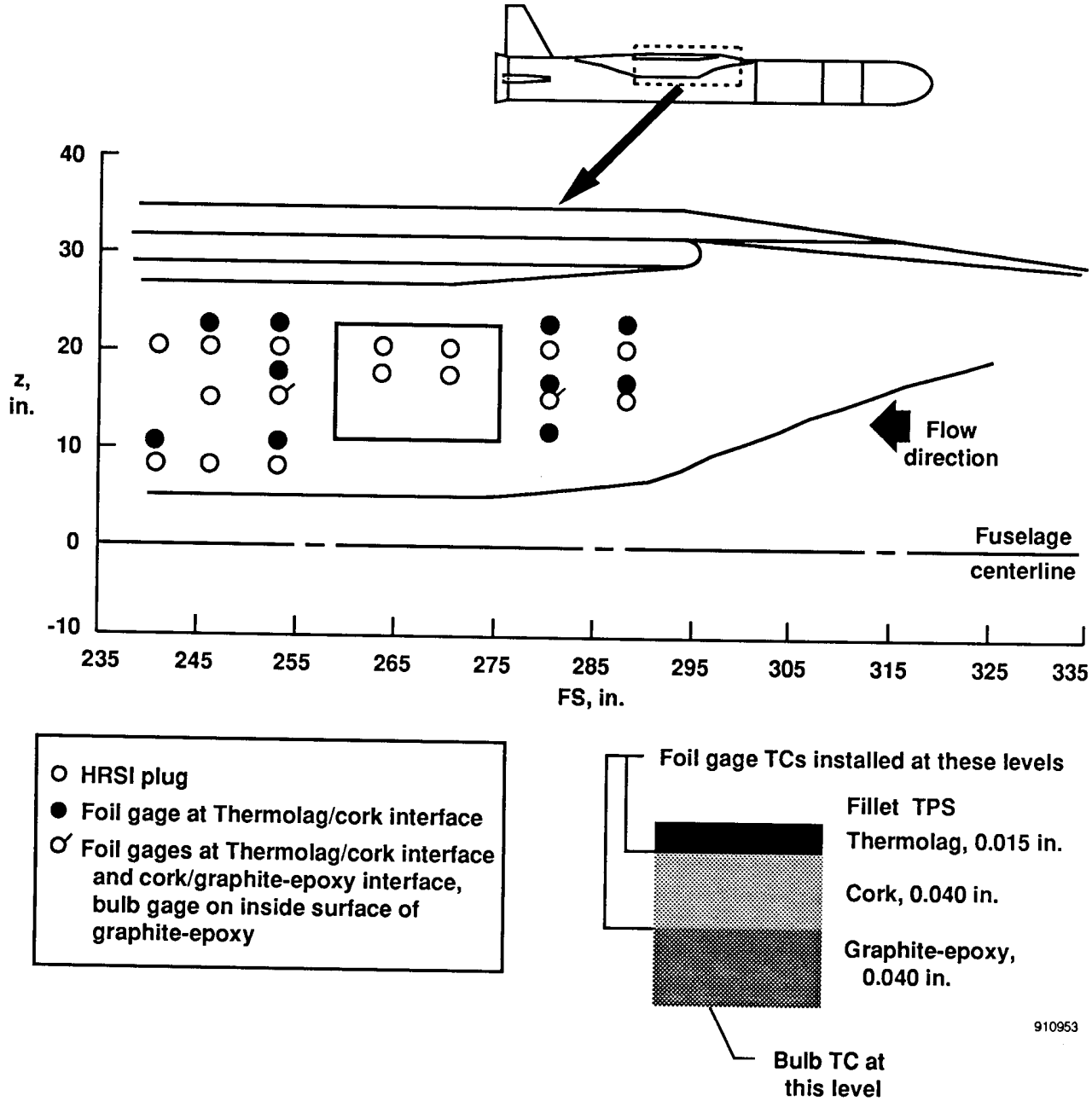

Fig. 5 Side view of wing-body fillet, showing temperature sensor locations.

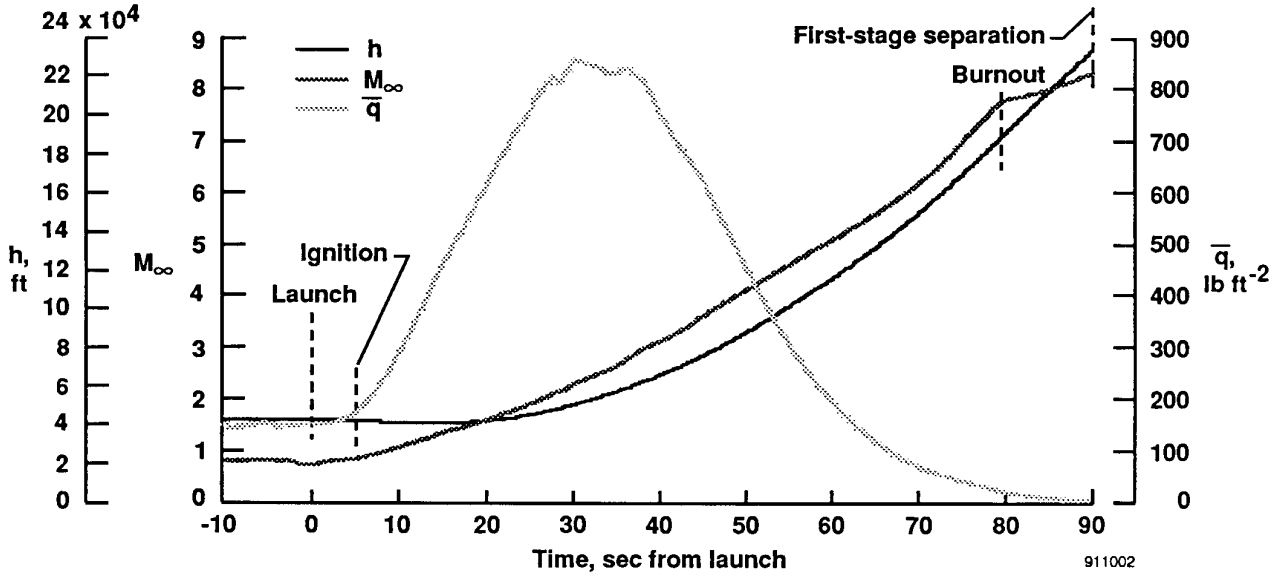

(a) Pressure altitude, free-stream Mach number, and free-stream dynamic pressure.

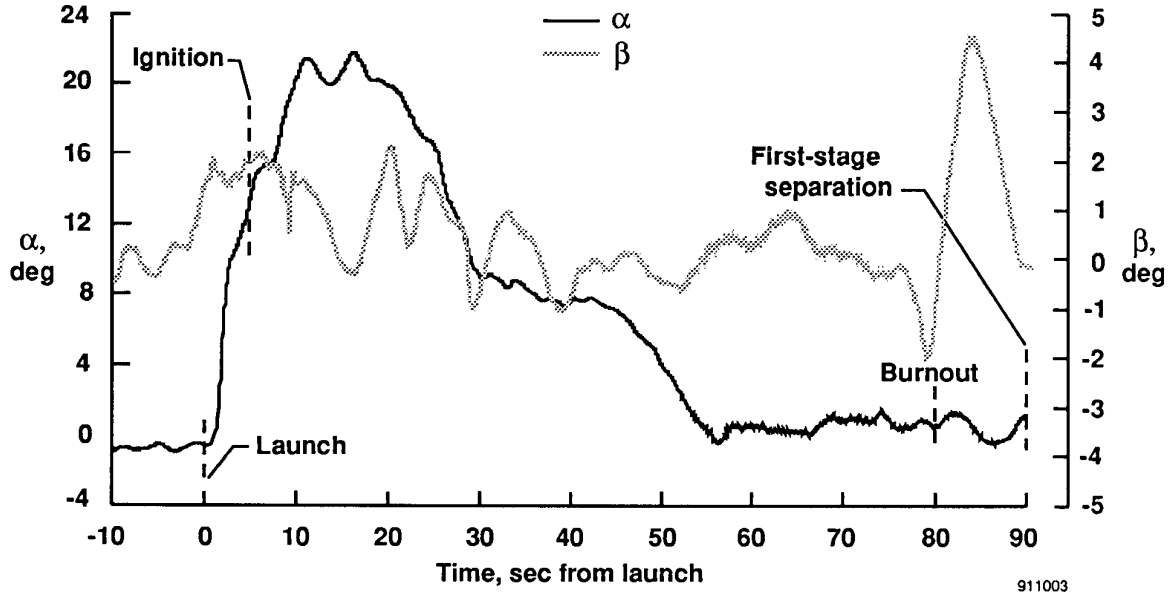

(b) Angle of attack and angle of sideslip.

Fig. 6 Pegasus flight trajectory time histories.

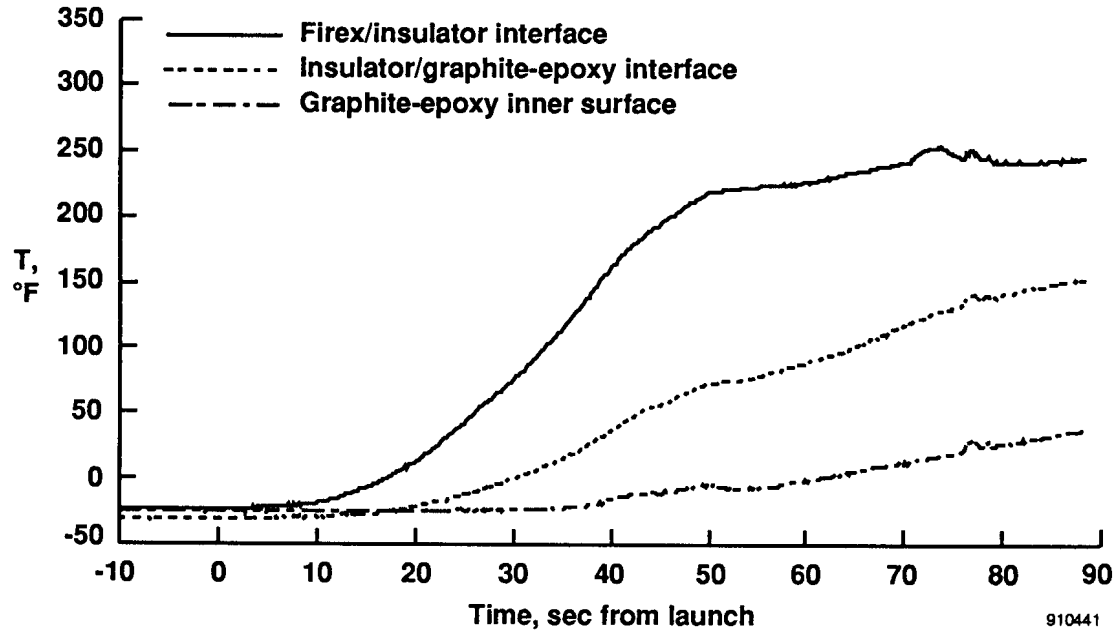

Fig. 7 Wing TPS interface temperatures, °F, FS = 293 in., y = 32 in.

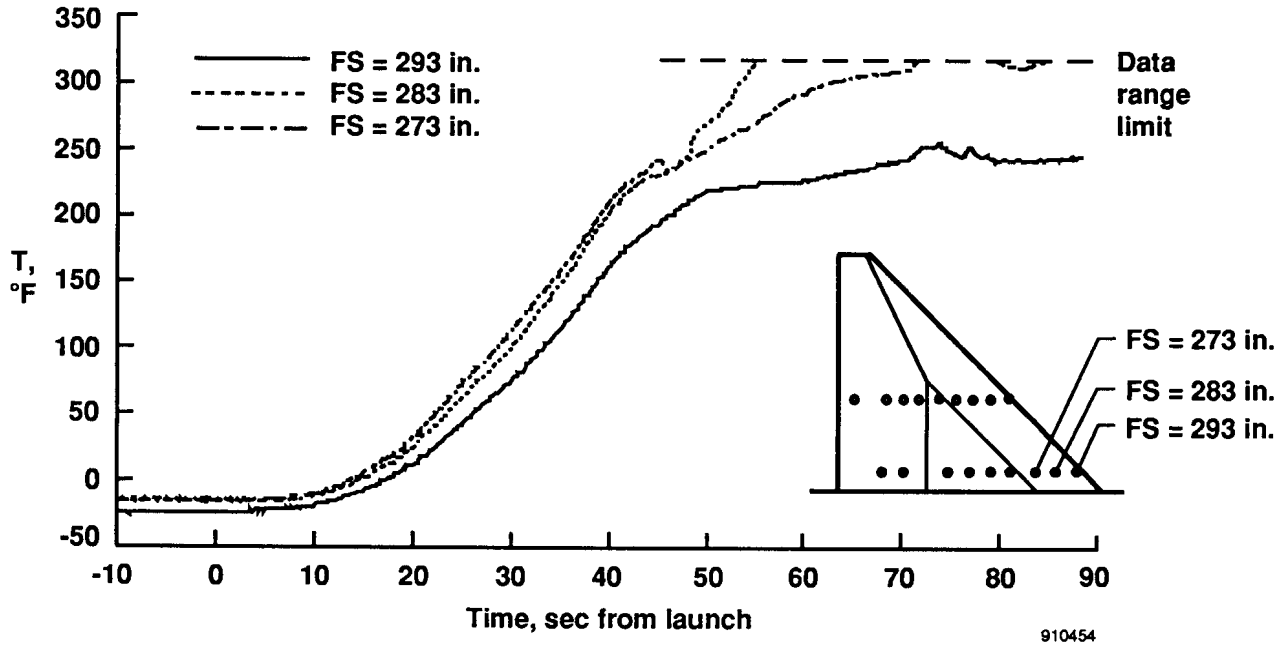

(a) FS = 293, 283, and 273 in.

Fig. 8 Lower surface wing temperature time histories, inboard row (y = 32 in.), Firex–insulator interface, °F.

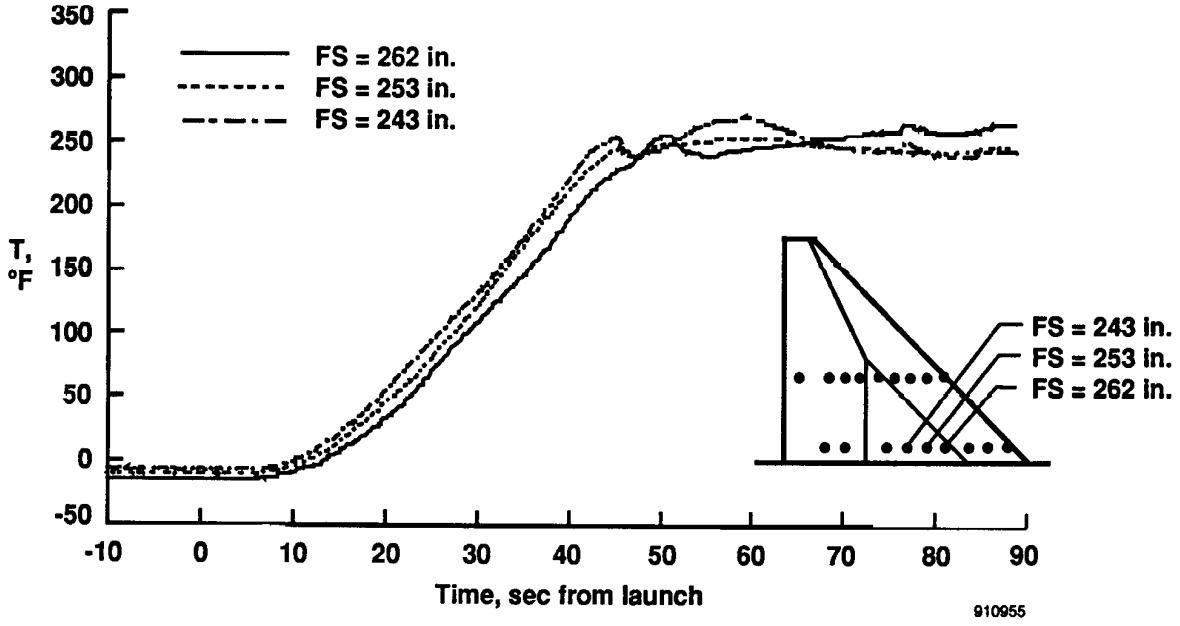

(b) FS = 262, 253, and 243 in.

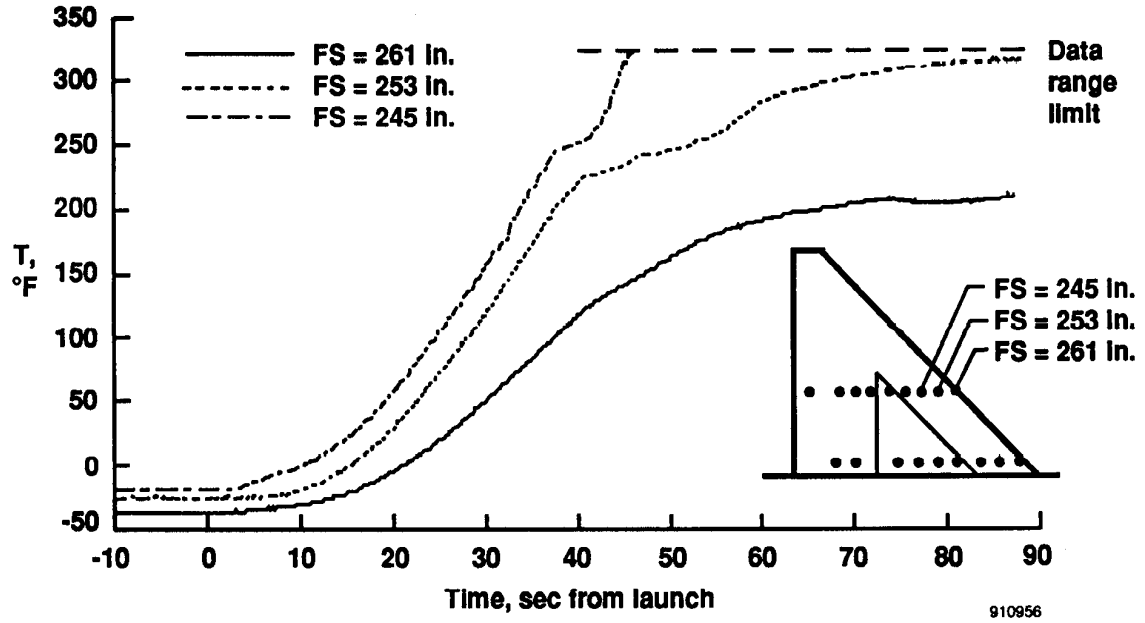

(c) FS = 261, 253, and 245 in.

Fig. 8 Continued.

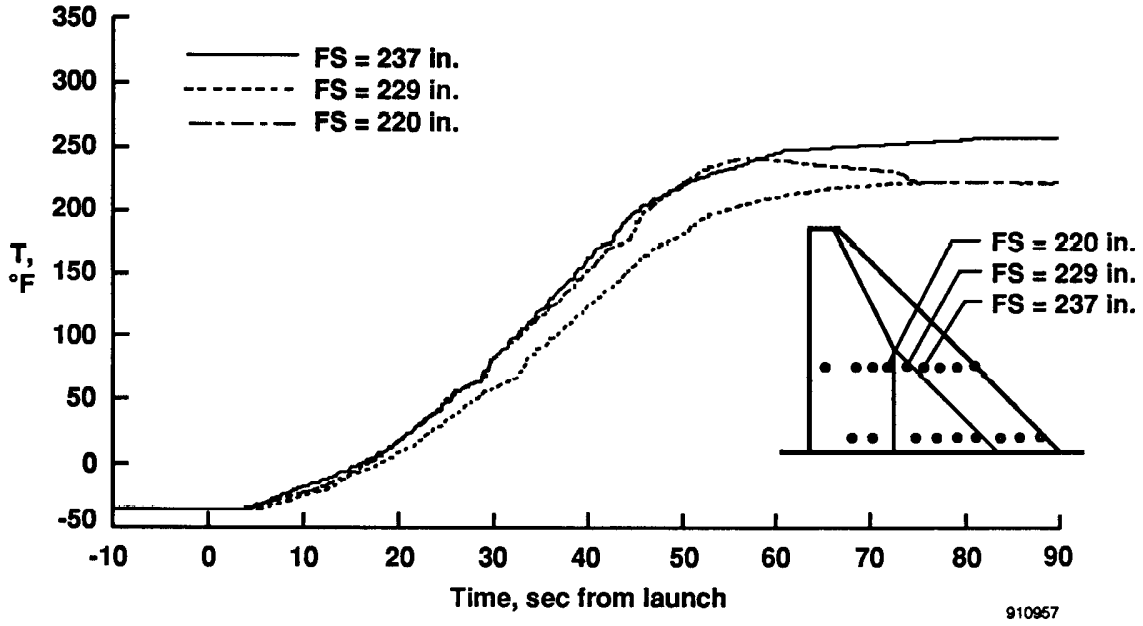

(d) FS = 237, 229, and 220 in.

Fig. 8 Concluded.

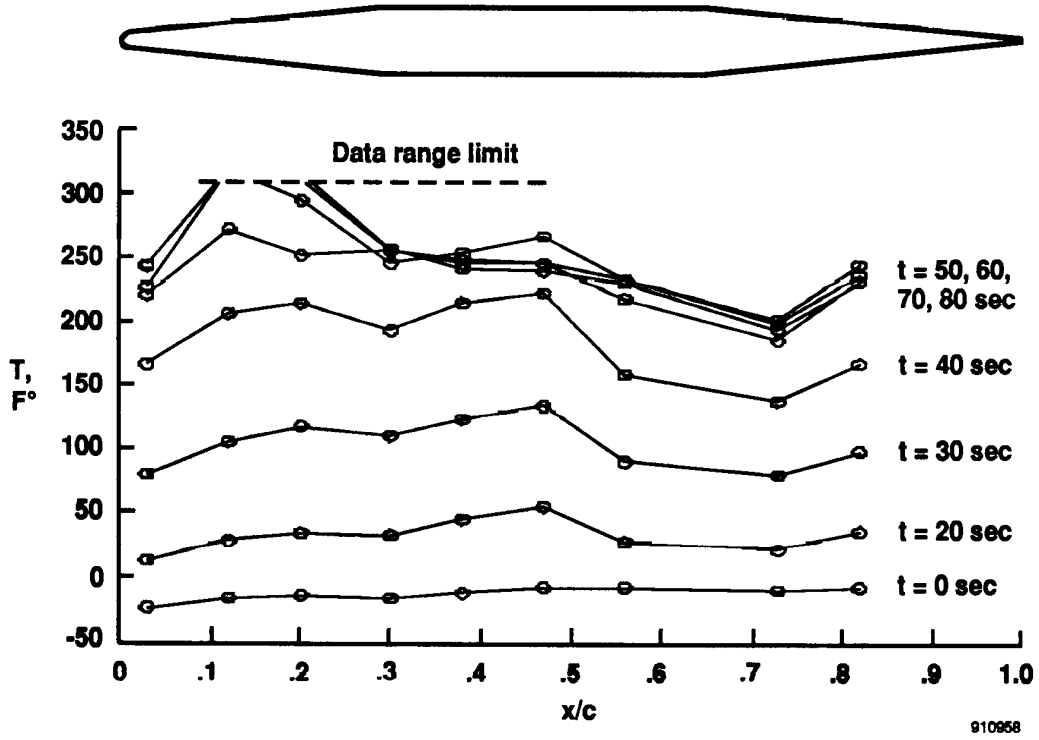

(a) Inboard row, $y = 32$ in.

Fig. 9 Chordwise distribution of wing lower surface temperatures at the Firex–insulator interface, °F.

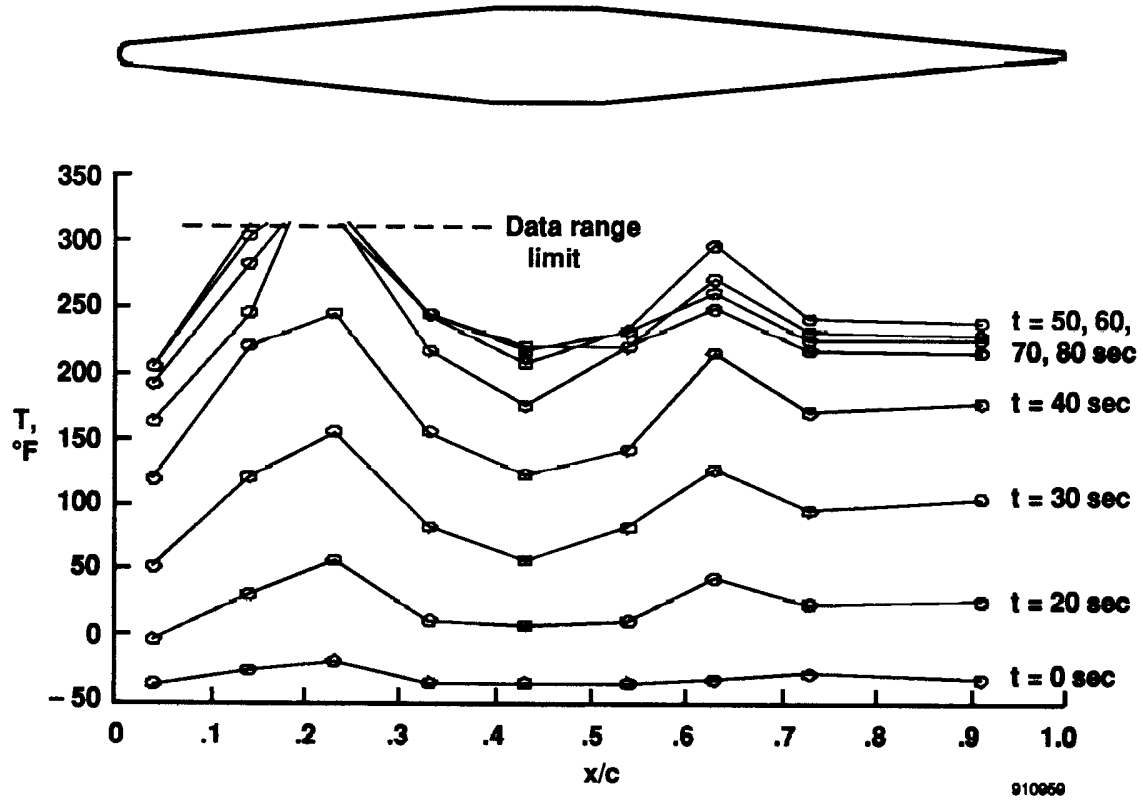

(b) Outboard row, $y = 65$ in.

Fig. 9 Concluded.

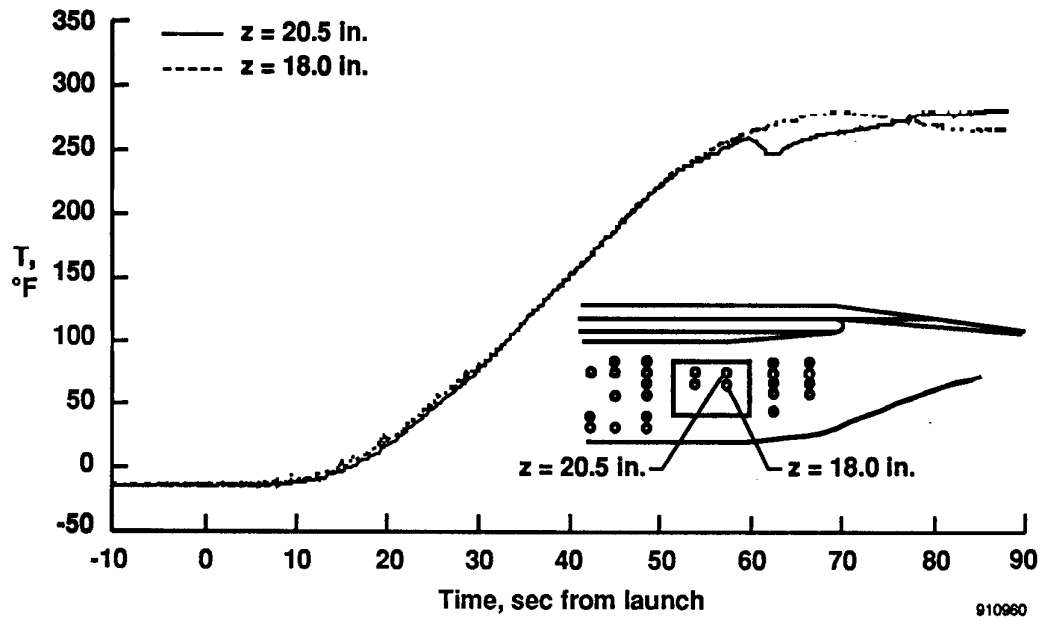

(a) FS = 270.4 in.

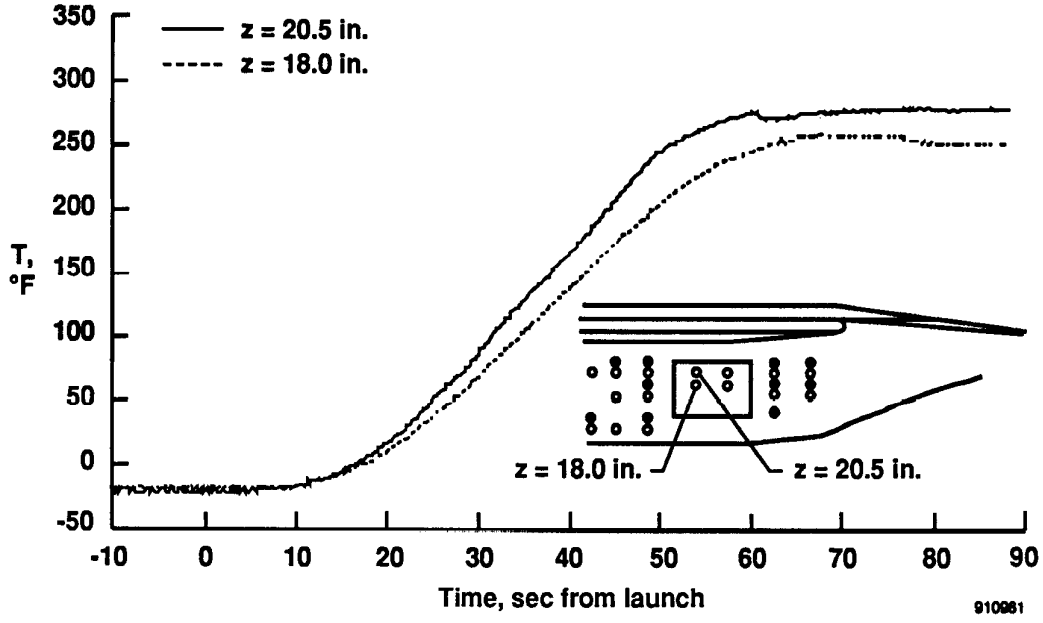

(b) FS = 263.5 in.

Fig. 10 Examples of fillet temperature time histories at the Thermolag–cork interface, °F.

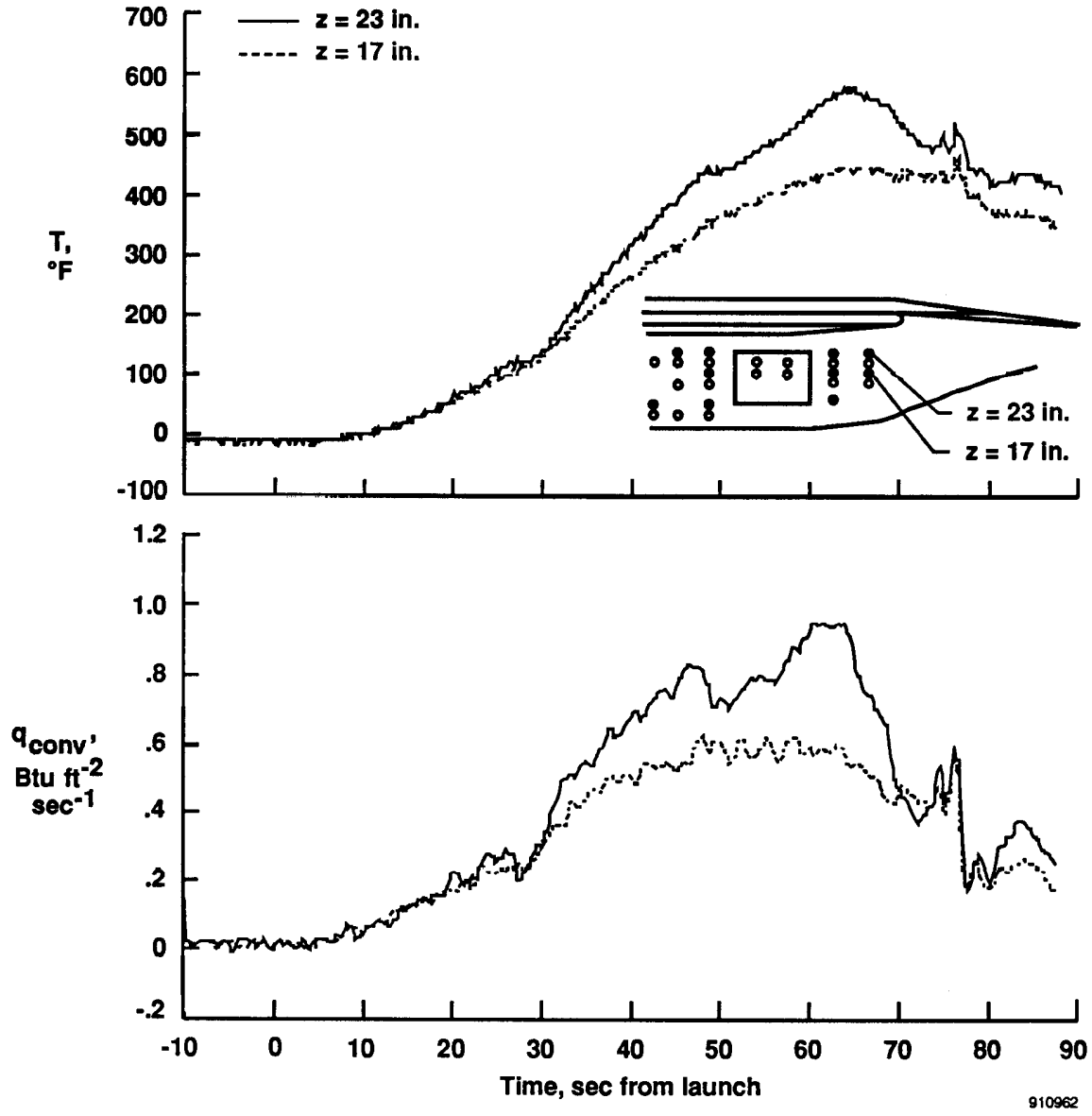

Fig. 11 HRSI plug surface temperature data and derived heat flux estimates at two locations, FS = 288.4 in.

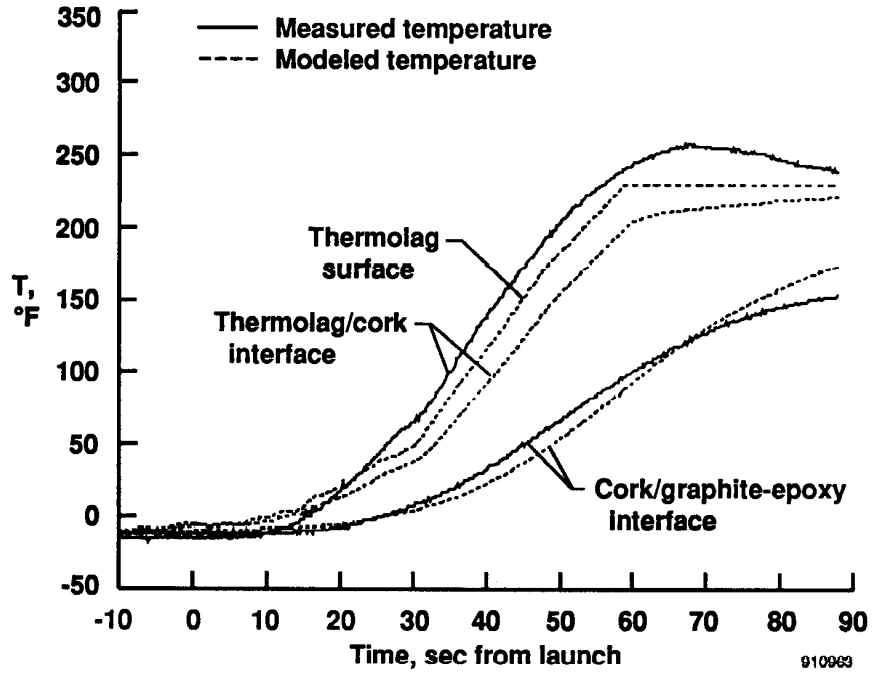

Fig. 12 Typical comparison of calculated TPS temperatures with measured flight data.

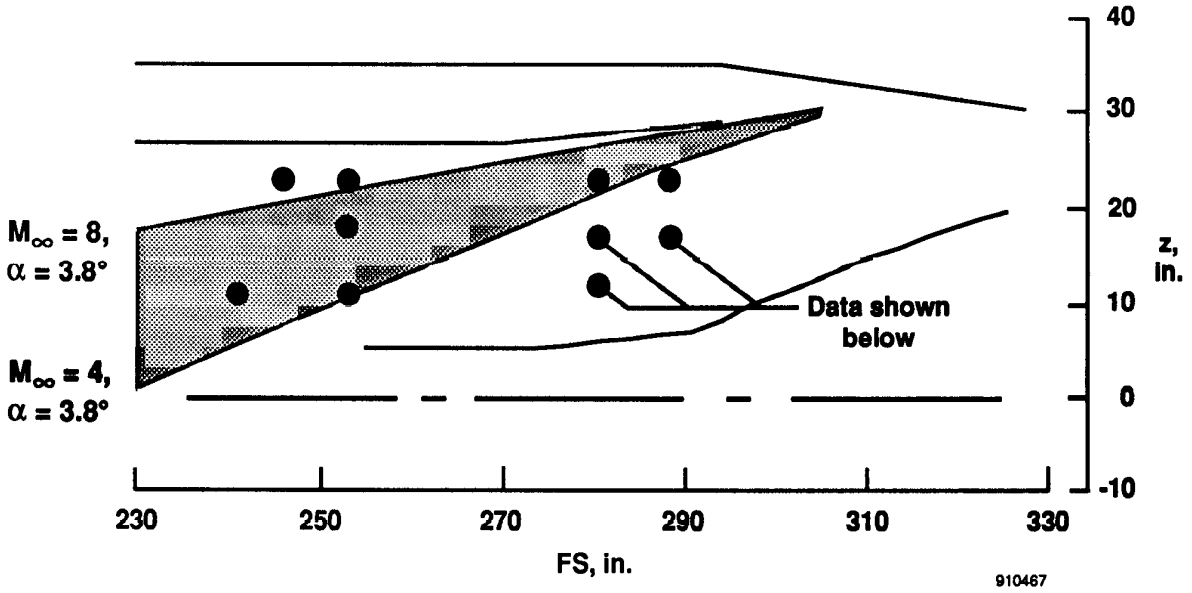

(a) Estimated wing leading-edge shock location, projected on fillet sidewall, two-dimensional wedge theory.

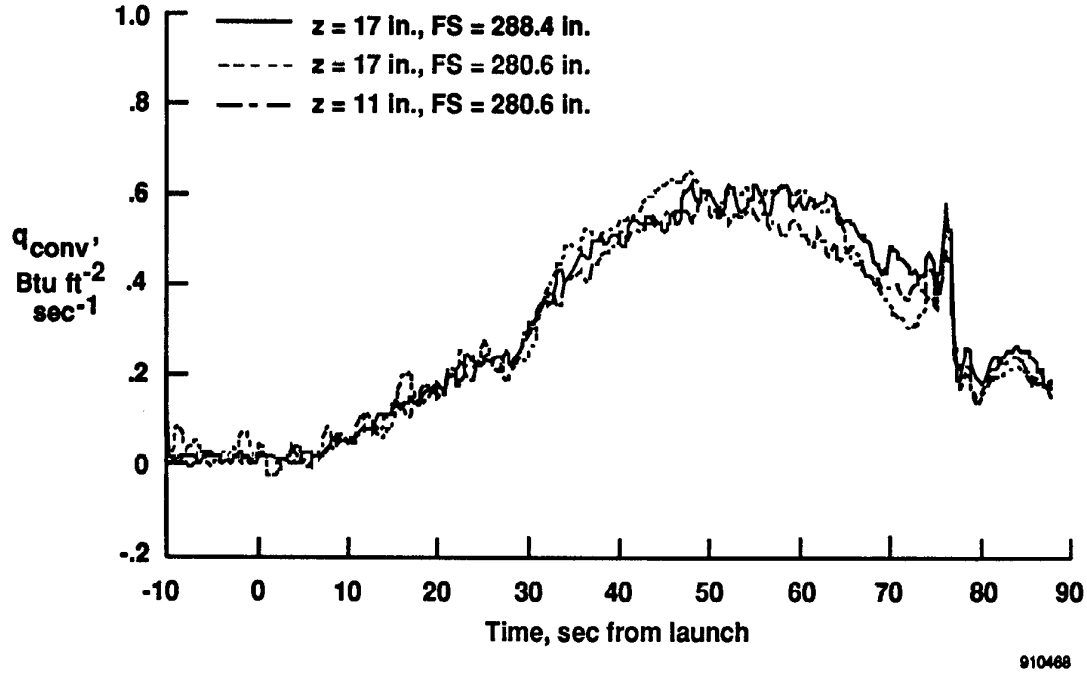

(b) Comparison of heat flux data, forward of estimated shock position.

Fig. 13 Fillet sidewall reference heating.

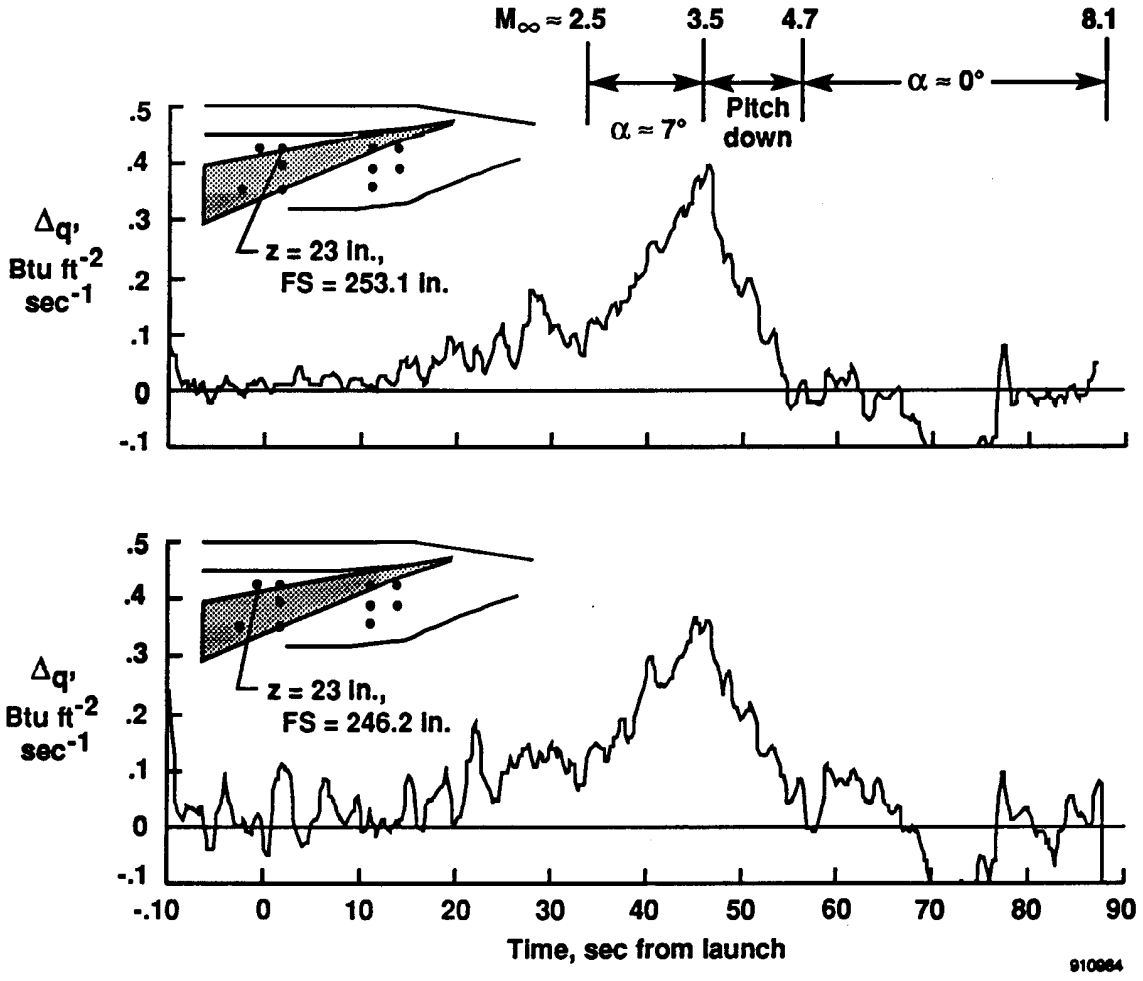

Fig. 14 Fillet sidewall heating, aft of shock.

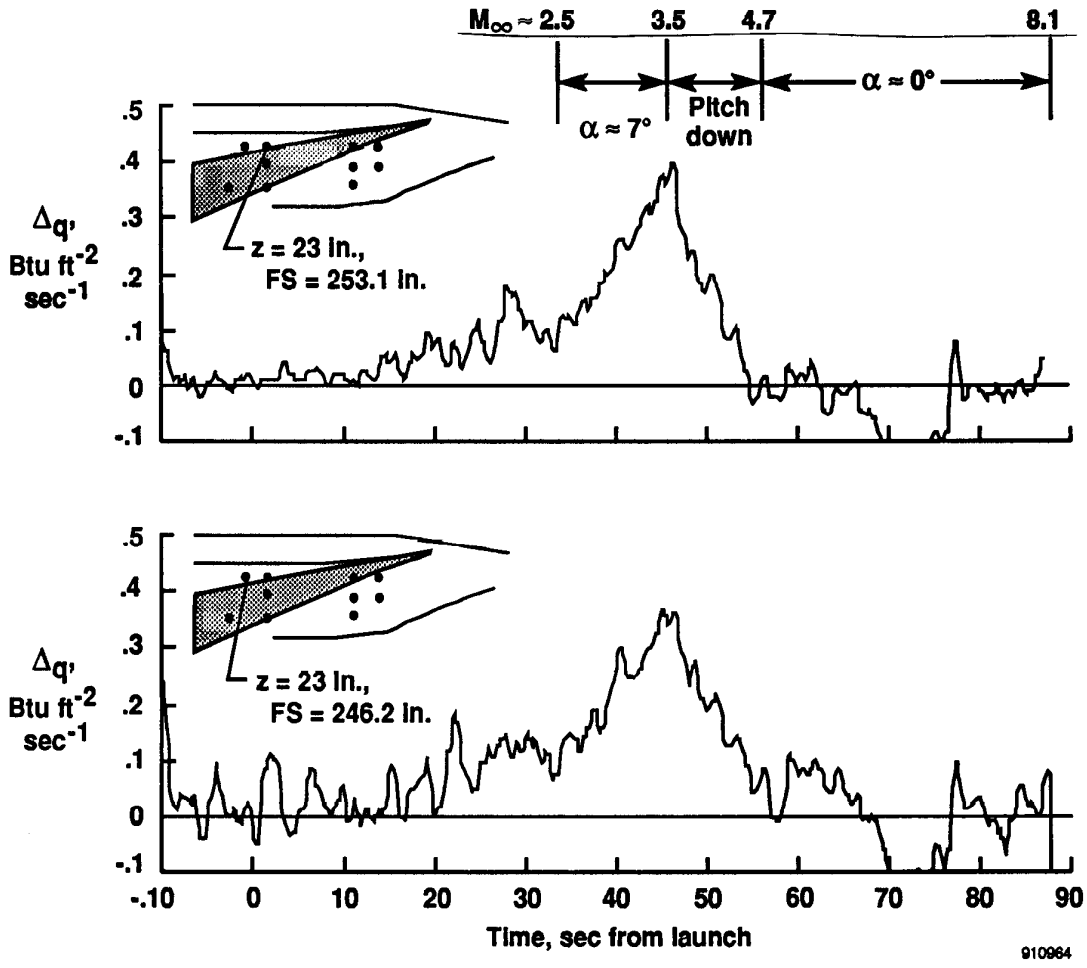

Fig. 14 Fillet sidewall heating, aft of shock.

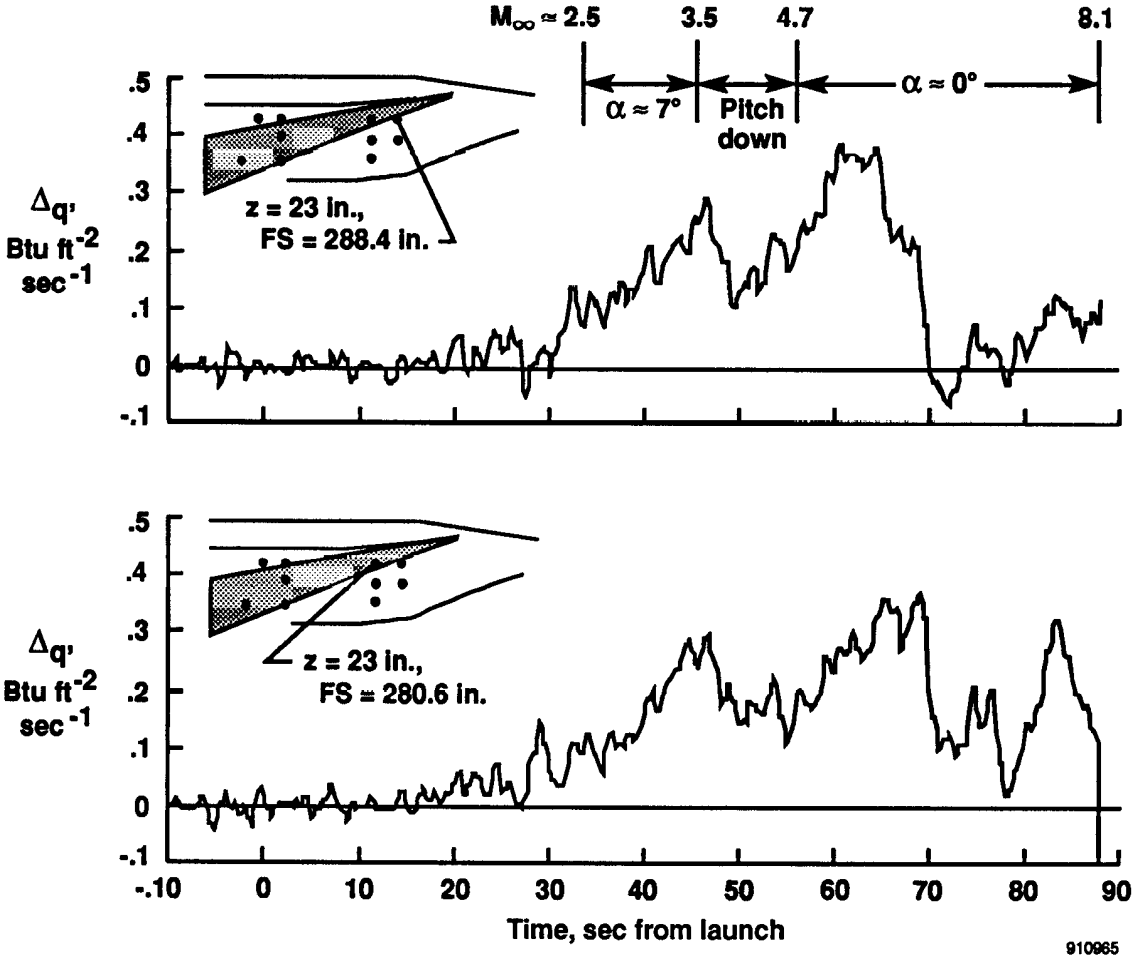

(a) FS = 288.4 in., z = 23 in.; FS = 280.6 in., z = 23 in.

Fig. 15 Fillet sidewall heating in the vicinity of the wing leading-edge shock at various locations.

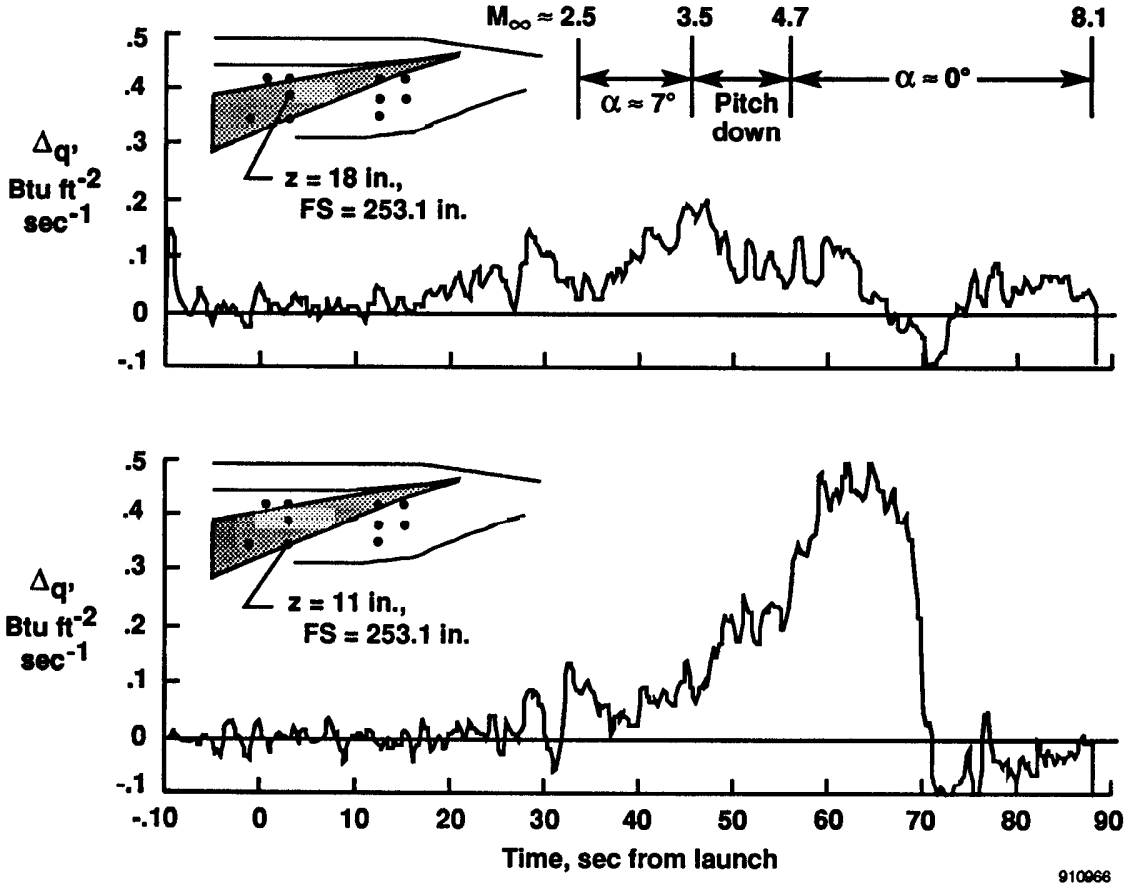

(b) FS = 253.1 in., z = 18 in.; FS = 253.1 in., z = 11 in.

Fig. 15 Continued.

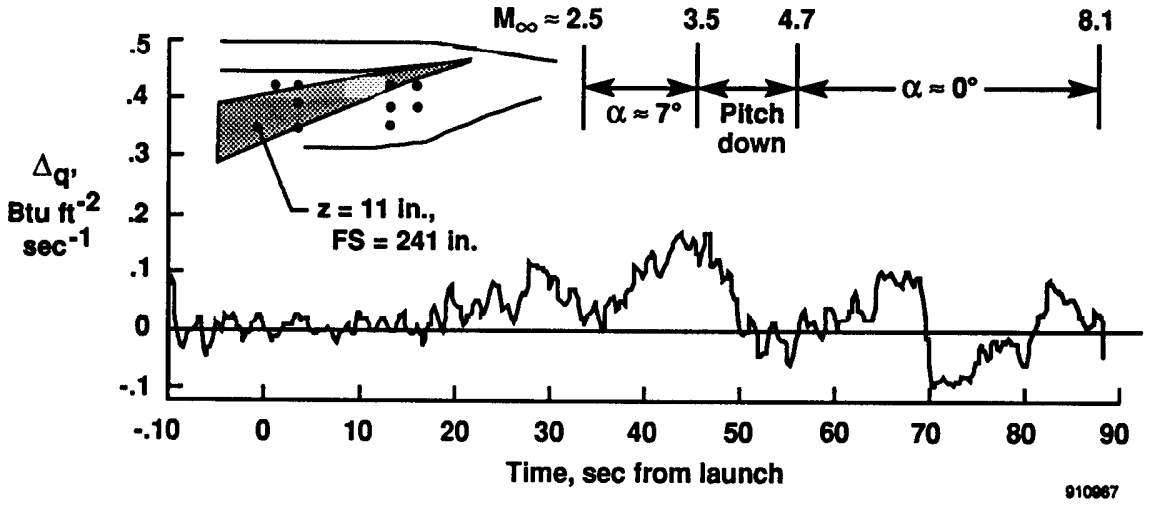

(c) FS = 241.0 in., z = 11 in.

Fig. 15 Concluded.